

RESEARCH REPORT

# Full-Field Optical Coherence Tomography of Human Donor and Pathological Corneas

Wajdene Ghouali<sup>1,2,3</sup>, Kate Grieve<sup>1,2,4</sup>, Salima Bellefqih<sup>3</sup>, Otman Sandali<sup>3</sup>,  
Fabrice Harms<sup>4</sup>, Laurent Laroche<sup>1,2,3</sup>, Michel Paques<sup>1,2,3</sup> and Vincent Borderie<sup>1,2,3</sup>

<sup>1</sup>Institut de la Vision, UPMC Univ Paris 06, UMR\_S 968, Paris, F-75012, France, <sup>2</sup>INSERM, U968, Paris, F-75012, France, <sup>3</sup>Centre Hospitalier National d'Ophthalmologie des Quinze-Vingts, INSERM-DHOS CIC 503, Paris, F-75012, France, and <sup>4</sup>Institut Langevin, 1 rue Jussieu, 75005 Paris, France

## ABSTRACT

**Purpose:** To evaluate the performance of a full-field optical coherence tomography (FF-OCT) system in the study of human donor and pathological corneas and assess its suitability for use in eye banks.

**Methods:** Our study was carried out using an FF-OCT system developed for non-invasive imaging of tissue structures in depth with ultrahigh resolution (1  $\mu$ m in all directions). Images were acquired from eight stored human donor corneas (either edematous or after deswelling) and five surgical specimens of corneas with various diseases (bullous keratopathy, lattice corneal dystrophy, stromal scar after keratitis, keratoconus and Fuchs dystrophy). They were compared with standard histology and pre-operative spectral domain OCT.

**Results:** The FF-OCT device enabled a precise visualization of the cells and the different structures (epithelium, basement membrane, Bowman's layer, stroma, Descemet's membrane and endothelium) in normal corneas. Specific lesions in various corneal diseases could also be easily identified, such as corneal edema, epithelium and Bowman's layer irregularities, breaks, or scars (keratoconus), stromal opacities, deposits, fibrosis (stromal corneal scar, bullous keratopathy, lattice corneal dystrophy) and Descemet's membrane thickening and guttae (Fuchs dystrophy). FF-OCT image features were comparable to the details provided by conventional histology. Higher resolution could be demonstrated with FF-OCT when compared with spectral domain OCT.

**Conclusion:** FF-OCT is a powerful non-invasive imaging tool that allows detailed study of corneal structures. Images correlate well with conventional histology. Further studies should evaluate the benefit of this technique as a complement to current assessment methods of human donor corneas.

**Keywords:** Corneal imaging, corneal storage, corneal transplantation, optical coherence tomography

## INTRODUCTION

Corneal diseases are considered the second major cause of blindness in developing countries.<sup>1</sup> Since the first corneal graft performed in 1905, many advances have been made thanks to the development of eye banks. An eye bank is an institution whose role is to collect and process donor corneas, and then distribute corneal grafts to surgeons.<sup>2–4</sup> Indeed, the quality of the donor corneal tissue plays an important role in the outcome of the transplantation procedure. Microbiological safety and quality of the tissue are

the main parameters on the “check-list” of corneal grafts. Optical or specular microscopy, with a detailed view of the corneal endothelium and cell density determination, remain the “gold standard” in the anatomical study of corneal graft. However, there is currently a lack of an efficient method for studying both epithelium and stroma. These two corneal layers also play a major role in the outcome of the graft. Assessment of the corneal epithelium is of importance, firstly, for measurement of topography, which can provide evidence of keratoconus or refractive surgery in the donor cornea.<sup>5</sup> Secondly, assessment of

the corneal epithelium is useful for gauging epithelium intactness. Indeed, abnormalities of the external surface of the corneal graft are an important cause of graft failure.<sup>6</sup> Abnormal corneal epithelium could result in persistent epithelial defect, thus leading to severe complications, such as scarring, infection, vascularization or perforation and eventually graft failure.<sup>7</sup> Finally, incidence of stromal opacities in donor corneas is significant in terms of tissue qualification and transplant.<sup>8</sup>

Optical coherence tomography (OCT)<sup>9</sup> is a non-invasive imaging modality analogous to ultrasound that uses interference of light to perform high-resolution cross-sectional study of biological samples. OCT imaging is now a well-established technique for *in vivo* imaging of the retina<sup>10</sup> and the anterior segment<sup>11</sup> at 5–15  $\mu\text{m}$  resolution. It provides good visualization in the cross-sectional view of the layered structures of these tissues.

A variant on the conventional (time or spectral domain) OCT technique called full-field optical coherence tomography (FF-OCT) offers microscopic resolution of 1  $\mu\text{m}$  in three dimensions using a white light source,<sup>12,13</sup> providing a cellular level view similar to histology, but without the need for fixatives or stains. Views of both the “en face” planes (i.e. same orientation as confocal microscopy) and cross-sections (i.e. same orientation as OCT or histology) are provided by the FF-OCT 3D data sets at high resolution. FF-OCT has been previously used to visualize corneal tissues.<sup>13–16</sup> The aim of this study was to evaluate the performance of FF-OCT in the non-invasive assessment of human donor corneas and to explore its efficiency in detecting corneal diseases.

## MATERIALS AND METHODS

This study was performed at the French National Eye Hospital (Centre Hospitalier National d’Ophtalmologie des Quinze-Vingts, Paris, France) in accordance with the declaration of Helsinki. It was approved by the Ethics Committee of the French Society of Ophthalmology. Subjects were informed of the aim of the study and all consents were obtained.

### Human Corneas

A total of 13 human corneas were used. The “normal” and “edematous” corneas were obtained from the tissue bank of Etablissement Français du Sang – Ile-de-France (Paris, France). These eight specimens were discarded before transplantation, according to the standards of the European Eye Bank Association, because of low endothelial cell count. Donor corneas were stored in organ culture as previously described.<sup>17</sup> Storage in organ culture medium

(CorneaMax, Eurobio, France) leads to corneal swelling, which gives a physiopathological model of edematous cornea. Organ-cultured corneas are issued for transplantation after deswelling in a specific medium containing Dextran (CorneaJet, Eurobio, France), resulting in grafts of normal thickness.

Surgical specimens of five diseased corneas (i.e. bullous keratopathy, lattice corneal dystrophy, stromal scar after infectious keratitis, keratoconus and Fuchs dystrophy) were obtained at the time of keratoplasty and stored in the deswelling medium used for the graft. They were imaged following surgery, immersed six hours in deswelling medium, and then fixed in formaldehyde (10%) for histopathology.

### FF-OCT Device

The experimental arrangement of FF-OCT (Figure 1A) is based on a configuration that is referred to as a Linnik interferometer.<sup>18</sup> A halogen lamp is used as a spatially incoherent source to illuminate the whole field of an immersion microscope objective. The signal is extracted from the background of incoherent back-scattered light using a phase-shifting method implemented in custom-designed software. This study was performed on a commercial FF-OCT device (LightCT, LLTech, Paris, France). This FF-OCT microscope is housed in a compact setup (Figure 1B) that is about the size of a standard optical microscope (310  $\times$  310  $\times$  800 mm L  $\times$  W  $\times$  H).

FF-OCT provides the highest OCT 3D resolution of 1  $\times$  1  $\times$  1  $\mu\text{m}^3$  (X  $\times$  Y  $\times$  Z) on unprepared label-free tissue samples over a wide field of view that allows digital zooming down to the cellular level.<sup>13</sup> In contrast to conventional OCT, it produces “en face” images in the native field view, similar to confocal microscopy images (i.e. with similar lateral yet superior axial resolution), and the cross-sectional views are then reconstructed from the 3D data stack. It combines attributes of confocal and OCT techniques to provide both high-resolution “en face” and cross-sectional views in a single instrument. FF-OCT image acquisition and processing time is under five minutes for an 800  $\mu\text{m}$   $\times$  800  $\mu\text{m}$   $\times$  500  $\mu\text{m}$  depth stack in the cornea.

FF-OCT image contrast is generated by the same principles as in conventional OCT, i.e. it shows differences in light backscattering between the different tissue components, or in other words shows differences in refractive index. The most significant difference between FF-OCT and conventional OCT is the higher resolution achieved. The axial resolution improvement is thanks to the use of a white light source illuminating the whole field as compared to a laser source scanning the field point by point. This in turn means that microscope objectives may be used to

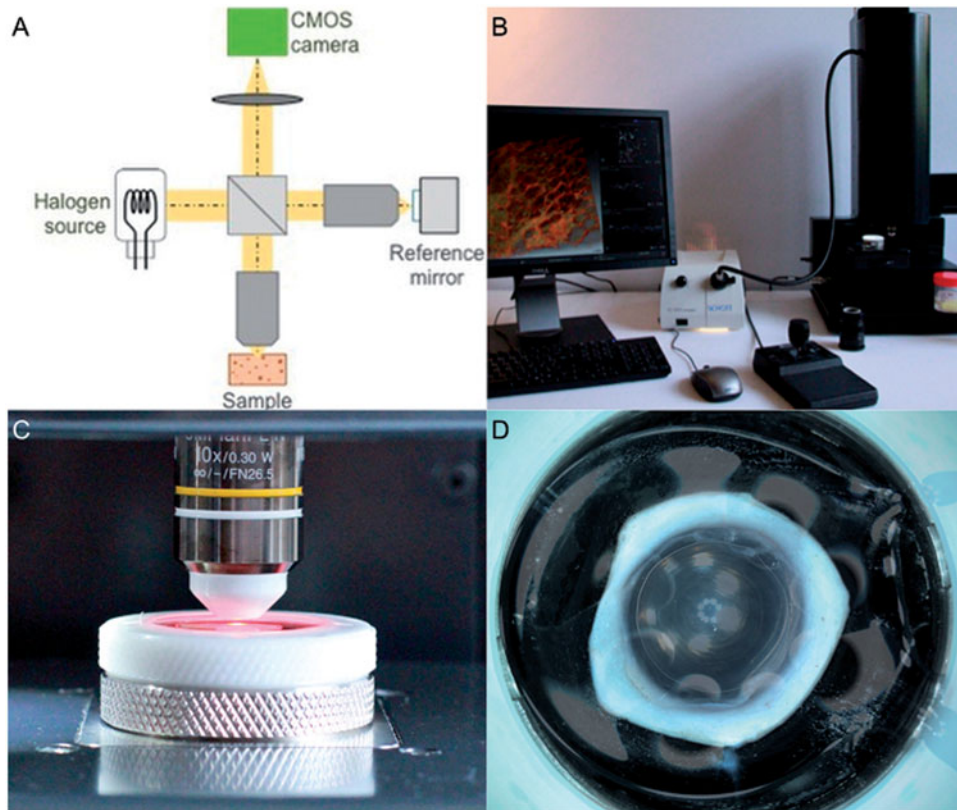


FIGURE 1 Experimental setup and photographs of the FF-OCT device. (A) Schematic of the optical setup; (B) photograph of the device; (C) zoom on the sample holder; (D) photograph of a cornea in the holder.

improve transverse resolution (possible due to the reduced depth of field in FF-OCT, and hence implying a trade-off of reduced penetration depth), and image capture of the whole field can be performed in a single shot by a complementary metal-oxide semiconductor (CMOS) camera as opposed to a single pixel detector. The resulting native image orientation is therefore “en face” in FF-OCT versus cross-sectional in conventional OCT. These technical factors result in resolution of  $1\ \mu\text{m}$  3D versus around  $5\text{--}15\ \mu\text{m}$  3D in conventional OCT. Penetration depth in FF-OCT is around  $1\ \text{mm}$  in cornea versus over  $1\ \text{mm}$  in most tissues with conventional OCT. It should be noted that the acquisition speed of FF-OCT is limited by currently available CMOS camera technology, and is at present too slow to allow *in vivo* corneal imaging, whereas conventional OCT is routinely used for *in vivo* examinations. The technique is therefore suited to applications where *ex vivo* tissues must be examined, as in the current example of donor corneas.

### Image Acquisition

Stacks of  $800\ \mu\text{m} \times 800\ \mu\text{m}$  “en face” images were captured on each cornea in the central zone. Optical slices were acquired in  $1\ \mu\text{m}$  steps through the entire corneal depth, resulting in a 3D data stack that could

be viewed in custom viewing software as “en face” still frames or movies, as reconstructed still frame or movie cross-sections or in a 3D volumetric rendering. Acquisition time from positioning the cornea in the sample holder to viewing the images was under five minutes for a typical  $800\ \mu\text{m} \times 800\ \mu\text{m} \times 500\ \mu\text{m}$  stack. The instrument can also acquire wide-field images by automated mosaicking of native fields. The sample is contained in a custom sample holder that can be sterilized.

### Histology

After FF-OCT images were acquired, corneas were fixed in formaldehyde (10%) and embedded in paraffin. Four micrometer sections were stained with Hematoxylin–Eosin–Safran (HES) or Periodic Acid Schiff (PAS) and observed with a light microscope.

### Spectral Domain OCT

A spectral-domain OCT system (RTVue; Optovue, Inc, Fremont, CA) with a corneal adaptor was used in this study. This device provides corneal images with an axial resolution of  $5\ \mu\text{m}$ . Spectral-domain OCT images were taken before keratoplasty.

## RESULTS

### FF-OCT of Organ-Cultured Corneas

Four organ-cultured human corneas were analyzed after deswelling in Dextran-containing medium. The different structures of the cornea (epithelium, basement membrane, Bowman's layer, stroma, Descemet's membrane and endothelium) could be clearly identified in all specimens. The corneal epithelium, basement membrane, keratocytes and endothelium were hyper-reflective, whereas Bowman's layer, stromal lamellae and Descemet's membrane were hypo-reflective. Figure 2 shows an axial section of an organ-cultured "normal cornea" (after deswelling) reconstructed from the 3D stack, in which "en face" slices were acquired at 1  $\mu\text{m}$  depth intervals. "En face" pictures (Figure 2B–F) allowed the visualization of successive layers in a manner comparable to confocal microscopy. Individual cells in the superficial, wing cell and basal epithelial cell layers were clearly distinguished, as were individual keratocytes in the stroma, and endothelial cells in their hexagonal pavement.

Four organ-cultured human corneas were analyzed before deswelling. Corneal edema was characterized by increased corneal thickness (1100  $\mu\text{m}$ ) due to excessive accumulation of water into hydrophilic stromal layers (Figure 3). As no light scattered in these regions, the absence of tomographic signal appeared as a dark region that was associated with a disorganization of the collagen lamellae.

### FF-OCT of Surgical Specimens

Intraepithelial edema and subepithelial fibrosis were clearly imaged in cross-sections and "en face" sections of a bullous keratopathy specimen (Figure 4). In a corneal specimen tissue from a lattice corneal dystrophy patient who underwent deep anterior lamellar keratoplasty, corneal opacities were well identified in both cross section and "en face" pictures as hyper-reflective structures predominant in the anterior stroma (Figure 5). In a corneal specimen tissue obtained from a patient who underwent deep anterior lamellar keratoplasty as a surgical treatment for stromal scar after infectious keratitis, the consequences of infectious keratitis were well identified on cross section and "en face" pictures as highly reflective structures corresponding to the corneal opacity that progressively decreased from the upper to the lower stroma (Figure 6). In a corneal specimen tissue obtained from a keratoconus patient who underwent deep anterior lamellar keratoplasty, irregularities of the epithelium and Bowman's layer thickness were easily identified (Figure 7). Stroma was also affected, with an alteration of the normal organization of collagen lamellae that had an undulated pattern. In a Descemet's membrane specimen obtained from a Fuchs dystrophy patient who underwent endothelial keratoplasty, longitudinal cross section showed typical excrescences of Descemet's membrane, while "en face" pictures showed typical dark areas corresponding to guttae (Figure 8).

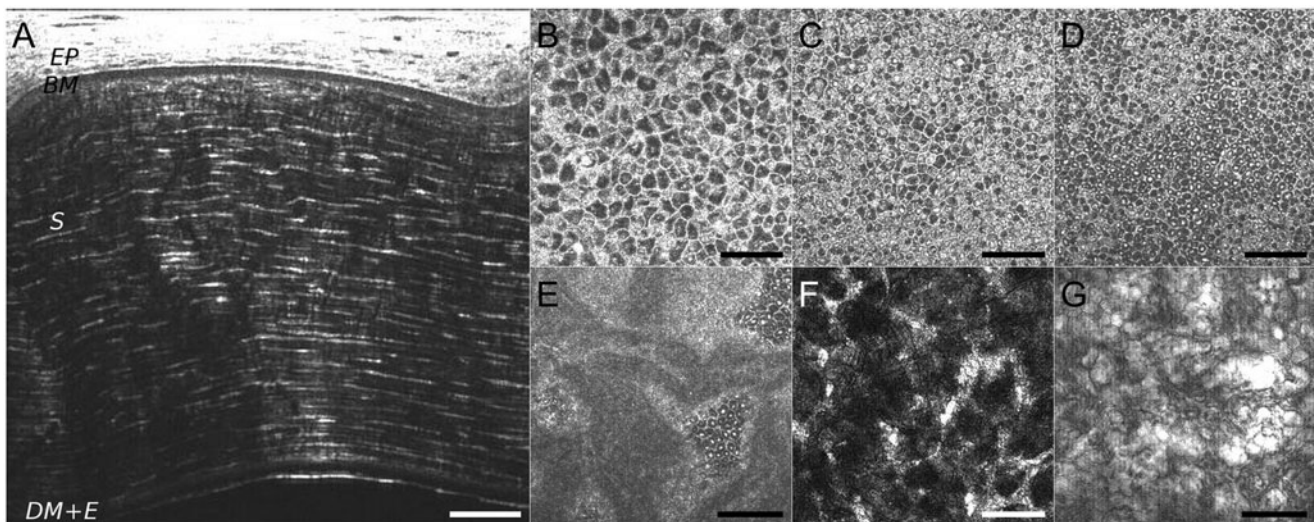


FIGURE 2 Organ-cultured normal cornea after deswelling in dextran-containing medium. (A) Cross-sectional slice with marked layers; EP, epithelium (38  $\mu\text{m}$  thick); BM, Bowman's layer (11  $\mu\text{m}$  thick); S, stroma (510  $\mu\text{m}$  thick); DM + E, Descemet's membrane (10  $\mu\text{m}$  thick) and endothelium. Bar shows 70  $\mu\text{m}$  in A, 100  $\mu\text{m}$  in B to G. B-G: "En-face" images. (B) Superficial epithelial layer. Superficial cells are either hyper-reflective or hypo-reflective and small nuclei can be observed. (C) Wing cell layer. (D) Basal epithelial layer. (E) Basal epithelial cells, basement membrane (hyper-reflective zones), and Bowman's layer (hypo-reflective zones). (F) Stromal keratocytes and lamellae of collagen bundles. (G) Endothelial cells revealed by decreasing axial resolution (sum of ten 1  $\mu\text{m}$  thick slices).

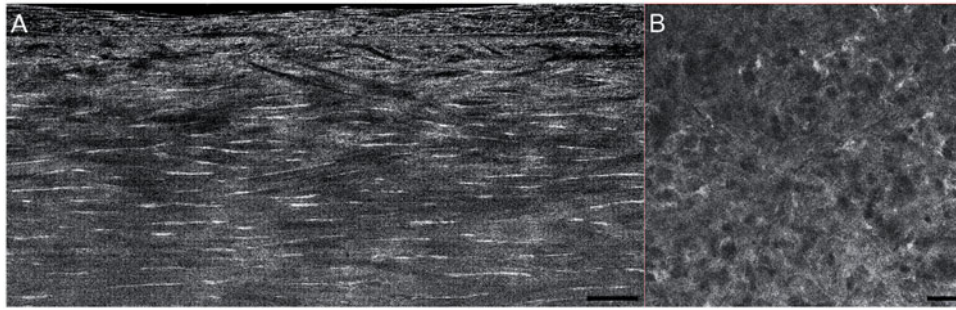


FIGURE 3 Organ-cultured normal cornea before deswelling (“edematous cornea”). (A) Cross-section of swelled cornea in organ culture medium, where lakes are seen as dark areas. Bar shows 50  $\mu\text{m}$ . (B) “En face” view, where lakes can be identified as dark areas, white keratocytes are sparse, and the corneal stroma has a general grey dense aspect. FF-OCT achieves penetration depths of several hundred microns in the presence of edema. Bar shows 100  $\mu\text{m}$ .

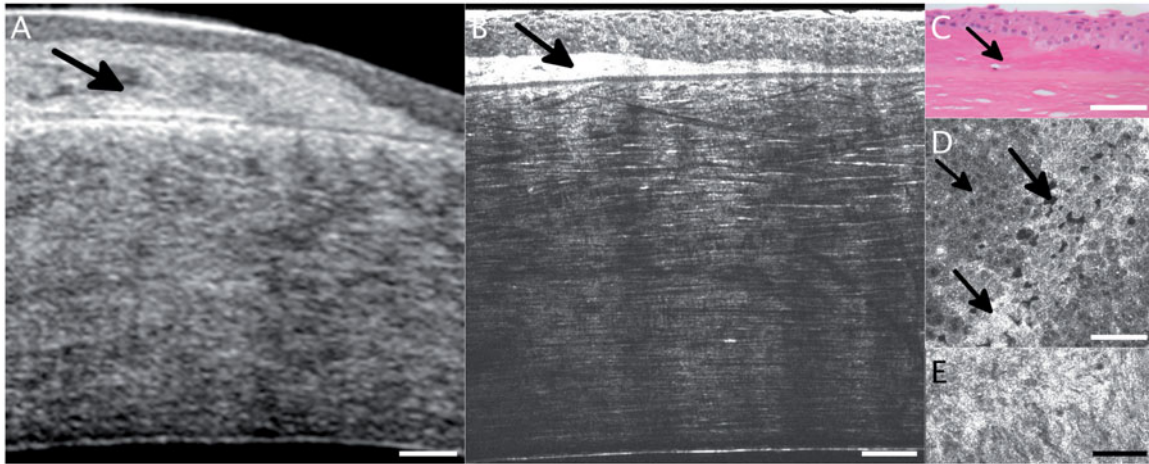


FIGURE 4 Bullous keratopathy. (A) Portion of a spectral domain OCT image of the cornea *in vivo* before keratoplasty. (B) Corresponding FF-OCT view of this area *ex vivo*. (C) Corresponding histology. The improvement in resolution between A and B can be appreciated, as can the correspondence of FF-OCT image B with histology C. Arrows in A, B and C indicate the area of sub-epithelial fibrosis. The epithelial thickness is normal where sub-epithelial fibrosis is moderate and decreases where sub-epithelial fibrosis is prominent. Bowman’s layer is clearly seen under the area of sub-epithelial fibrosis. (D) shows an “en face” FF-OCT view in the upper epithelium, where the arrows indicate intraepithelial edema that is seen as dark spaces (top arrow), grey wing cell layer (middle arrow) and bright surface epithelial cells (lower arrow). (E) shows an “en face” FF-OCT view located in the zone of subepithelial fibrosis, which appears as a bright white area. Scale bars show 200  $\mu\text{m}$  (A, B) and 100  $\mu\text{m}$  (C, D, E).

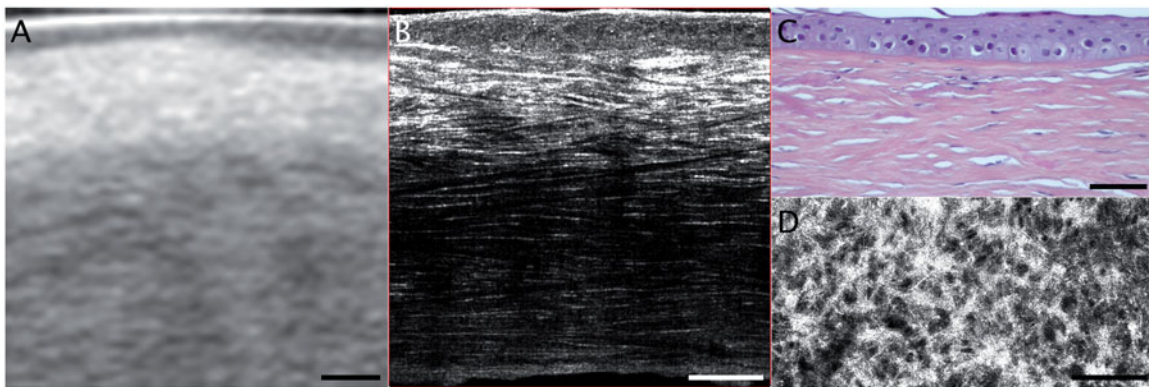


FIGURE 5 Lattice corneal dystrophy. (A) Portion of a spectral domain OCT image on the *in vivo* eye before keratoplasty. (B) Corresponding FF-OCT cross-section in the *ex vivo* cornea. (C) Corresponding histology. The high density of keratocytes in the upper stroma can be seen in cross sectional (B) and “en face” (D) FF-OCT views. The filament deposits below the epithelium can be seen in D. Scale bars show 200  $\mu\text{m}$ .

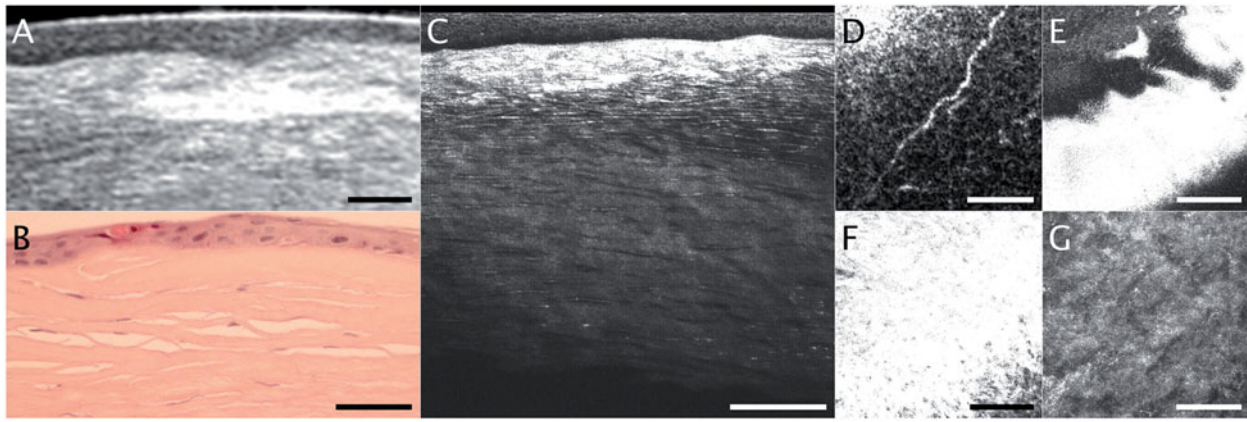


FIGURE 6 Stromal scar after infectious keratitis. (A) Portion of a spectral domain OCT image on the *in vivo* eye before keratoplasty. (B) Corresponding histology. (C) Corresponding FF-OCT cross-section in the *ex vivo* cornea. The scar region is visible as a hyper-reflective bright white region in the cross-section view (C) and “en face” FF-OCT views (E, F). Bowman’s layer is absent (B, C). D shows a subepithelial nerve in proximity to Bowman’s layer. The scar extends from the subepithelial region (E) into the stroma (F). Lower stroma (G) is also affected and shows abnormal lack of keratocytes and a dense grey aspect. Scale bars show 200  $\mu\text{m}$  (A, B, C); 50  $\mu\text{m}$  (D); 100  $\mu\text{m}$  (E, F, G).

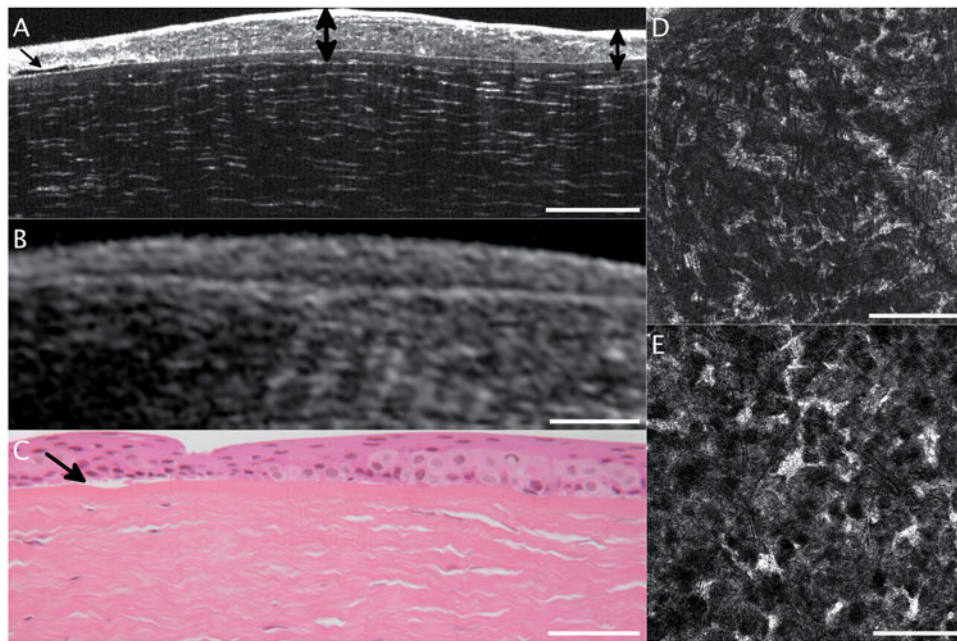


FIGURE 7 Keratoconus. (A) FF-OCT cross-section in the *ex vivo* cornea. (B) Portion of a spectral domain OCT image on the same eye *in vivo* before keratoplasty. (C) Histology of the same sample. The irregular thickness of Bowman’s membrane and the undulated arrangement of both the collagen lamellae and keratocyte layers are revealed. An epithelial scar can be seen to the far left in A and C (indicated by an arrow). Measurements on this image reveal a variability of Bowman’s layer thickness from edges to center (7  $\mu\text{m}$  to 12  $\mu\text{m}$ ) in comparison with Bowman’s membrane thickness in normal cornea (10  $\mu\text{m}$  to 12  $\mu\text{m}$ , as measured on the cornea of Figure 2). Epithelial thickness is also variable from edges to center in the keratoconus cornea: (39  $\mu\text{m}$  to 45  $\mu\text{m}$ ) in comparison with epithelial thickness in normal cornea (37  $\mu\text{m}$  to 40  $\mu\text{m}$ , again measured on the cornea of Figure 2). Locations of maximum and minimum thickness measurements are indicated by double-headed arrows in A. D shows an “en face” FF-OCT view in the upper stroma where keratocytes are numerous, small and arranged according to the undulated pattern of the layers. For comparison, E shows an “en face” FF-OCT image in upper stroma of normal cornea where keratocytes are more sparse, larger and arranged in flat layers. Scale bars show 100  $\mu\text{m}$  (A, B, C) and 200  $\mu\text{m}$  (D, E).

### Comparison of FF-OCT with Spectral Domain OCT and Histology

Higher resolution of FF-OCT images was evident compared with spectral domain OCT images in

all surgical specimens (Figures 4–8). Corneal pathology observed on FF-OCT images of surgical specimens obtained after surgery with no fixation and no staining was confirmed by conventional histology after fixation and appropriate staining.

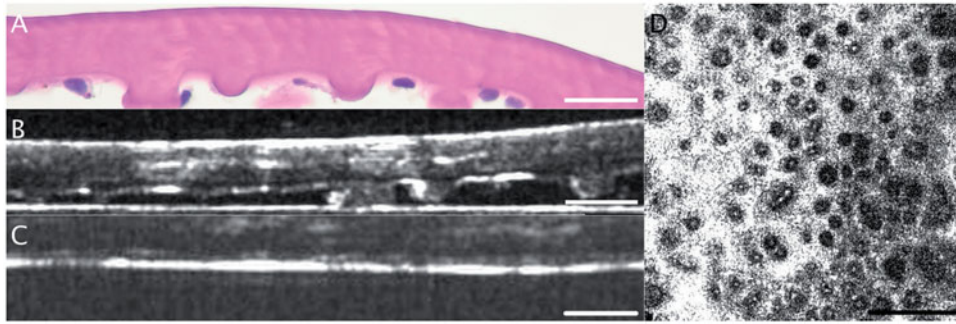


FIGURE 8 Fuchs dystrophy. (A) Histology of Descemet's membrane with Fuch's dystrophy. (B) FF-OCT cross-section in the same sample. Abnormal fibrosis and guttae beneath Descemet's membrane are visible. For comparison, (C) shows an FF-OCT cross-section in normal cornea. Thickness measurements on B and C reveal the thickening associated with Fuchs dystrophy: Descemet's membrane plus endothelial thickness in B is  $20\ \mu\text{m}$  on average compared to  $14\ \mu\text{m}$  in the normal cornea. Guttae are clearly visible in "en face" FF-OCT views (D), in a very similar manner to confocal microscopy. Scale bars show  $50\ \mu\text{m}$  (A, B, C) and  $100\ \mu\text{m}$  (D).

## DISCUSSION

We present here the first full-field OCT images of surgical specimens of human corneas with various diseases. Previous studies have shown the ability of the FF-OCT to identify the different structures in normal cornea,<sup>14,15</sup> thus demonstrating the strength of this technique for non-invasive study of the cornea. Our results complement the previous data, showing that normal corneal structures can be clearly visualized during graft storage, and specific lesions of corneal layers can be identified in a number of corneal diseases.

For *ex vivo* imaging, FF-OCT has advantages over both conventional OCT and confocal imaging. Axial  $\times$  lateral resolution is  $1\ \mu\text{m} \times 1\ \mu\text{m}$  in FF-OCT as compared to approximately  $5\ \mu\text{m} \times 15\ \mu\text{m}$  in conventional spectral domain OCT. Confocal imaging matches FF-OCT's lateral resolution of  $1\ \mu\text{m}$ , but axially is limited to  $5\text{--}20\ \mu\text{m}$ , so that cross-sectional views constructed from 3D confocal data sets appear blurred.

The study of the corneal endothelium is challenging with FF-OCT in comparison to confocal microscopy due to the superior resolution of FF-OCT. The endothelium may be clearly visible in cross-sectional views, but as the endothelium is not perfectly flat at the micron scale, the corresponding "en face"  $1\ \mu\text{m}$  thick slice will only reveal a few cells at a time in small regions of the field (cutting through stroma and Descemet's membrane in other regions). Indeed, the best conditions for revealing the endothelium are produced by imaging at the corneal summit where the layers will be as flat as possible with respect to the incident beam. If, however, a number of FF-OCT  $1\ \mu\text{m}$  thick "en face" slices are summed together, thereby simulating the resolution of a typical confocal instrument ( $5\text{--}20\ \mu\text{m}$ ), the pavement of horizontal endothelial cells appears more clearly across larger areas. Better images of endothelial cells with FF-OCT have been demonstrated in fresh corneas<sup>19</sup> (e.g. freshly

excised rat and mouse corneas). The corneas imaged in the current study were either stored and edematous or deswelled, or had been rejected for poor endothelial quality, so that it is not surprising that images of the endothelial layer show a less regular cellular pavement than *in vivo* confocal images of endothelium. Were FF-OCT imaging to be added to the donor cornea assessment process in the eye bank routine, the corneas would typically be assessed in a fresher state than that which was possible for the current study, meaning that better endothelial images could be expected. The endothelium is nevertheless not as well visualized either with FF-OCT or with confocal microscopy as with specular or light microscopy due to inevitable signal attenuation and increase in aberrations with depth. Normal procedure for endothelial examination in eye banks is by specular or light microscopy and FF-OCT, like confocal microscopy, does not seek to replace this.

This FF-OCT device is currently used for research in medical fields such as cancer surgery (rapid analysis of surgical margins<sup>20</sup> and sentinel nodes) and dermatology (differentiation between melanoma and carcinoma in real time without excision).<sup>21</sup> As no tissue preparation, modification or staining of any kind is needed for the imaging, this device appears suitable for the evaluation of human donor corneas considering the correlation between FF-OCT images and conventional histology pictures. Indeed, in current practice, aside from an excellent analysis of the corneal endothelium thanks to specular microscopy, the rest of the cornea is grossly observed with a slit-lamp. Fine details may escape the "check-list" and thus compromise the outcome of the corneal transplant. Lack of depth resolution in the slit-lamp view means that corneas may be rejected for stromal opacities that are in fact limited to anterior stroma or epithelial regions.<sup>8</sup> Such corneas could be designated to endothelial keratoplasty procedures. Lack of topography data with slit-lamp examination means that evidence of keratoconus or refractive surgery in

the donor may not be visible and may lead to graft failure.<sup>5,22-24</sup> Donor corneas that have been assessed by slit-lamp observation are stored with no digital image record of their structure. FF-OCT imaging automatically creates a digital image catalog of the corneas that have been assessed. Furthermore, in current practice, clinical history-taking of the donor might be incomplete and lack important details like history of refractive surgery or infectious keratitis. In this study, we clearly demonstrate the ability of the FF-OCT device to identify the different corneal structures in normal and diseased corneas. For instance, clear imaging of Bowman's layer enables detection of irregularities, breaks, scars or absence of this layer that are features of keratoconus, laser *in situ* keratomileusis, scars after infectious keratitis, or photorefractive keratectomy. These four corneal conditions, which are contra-indications for using donor tissue for penetrating or anterior lamellar keratoplasty, are currently difficult to detect in eye banks when the donor history is not precisely known. The fine assessment of the lamellar stroma, in terms of organization, number, thickness and reflectivity of the collagen lamellae and keratocyte density, provides a new means to assess the condition of the stroma in donor corneas and, potentially, its putative optical properties. This should be of major interest for selection of donor tissue for penetrating or anterior lamellar keratoplasty. Finally, Descemet's membrane can be precisely assessed with FF-OCT with regard to its thickness and structure. This information is certainly complementary to that provided by light and specular microscopy in the selection of donor tissue for penetrating or endothelial keratoplasty. Precise assessment of Descemet's membrane thickness could also be useful for selection of donor corneal tissue for Descemet's membrane endothelial keratoplasty, where thin Descemet's membrane may be more difficult to separate from the stroma.

Eye bank associations, such the Eye Bank Association of America or the European Eye Bank Association, have produced well-established medical and technical standards. Assessment of donor cornea is currently performed by the combined use of slit-lamp and specular or light microscopy. This process could be complemented by the addition of FF-OCT imaging, as it constitutes a powerful and non-invasive tool to complete the anatomical study of the cornea, especially the epithelium, Bowman's layer, stroma and Descemet's membrane. One limitation of our study is the sample size. The validation of the FF-OCT technique for routine use in eye banks requires further studies with its installation on-site and its use on a large series of donor corneas.

Development of the technique for *in vivo* imaging is limited by the acquisition speed of currently available and suitable CMOS cameras. Proof of principle of *in vivo* anterior segment FF-OCT imaging on rats has

been demonstrated.<sup>19</sup> *In vivo* FF-OCT endoscopy has also been demonstrated for imaging human skin.<sup>25</sup> Once faster camera technology becomes available, in future it may be possible to achieve *in vivo* imaging at a resolution level approaching that of the *ex vivo* instrument presented here.

## DECLARATION OF INTEREST

The authors report no conflicts of interest. The authors alone are responsible for the content and writing of this article.

Fabrice Harms is affiliated with LLTech SAS. Use of the LightCT Scanner was provided free of charge for the purpose of this study.

## REFERENCES

1. Tan DTH, Dart JKG, Holland EJ, Kinoshita S. Corneal transplantation. *Lancet* 2012;379:1749–1761.
2. Chu W. The past twenty-five years in eye banking. *Cornea* 2000;19:754–765.
3. Armitage WJ. Assessment of corneal quality by eye banks. *J Ophthalmic Vis Res* 2012;6:3–4.
4. Linke SJ, Eddy MT, Bednarz J, Fricke OH, Wulff B, Schröder AS, et al. Thirty years of cornea cultivation: long-term experience in a single eye bank. *Acta Ophthalmol* 2013;91:571–578.
5. Stoiber J, Ruckhofer J, Hitzl W, Grabner G. Evaluation of donor tissue with a new videokeratoscope: the Keratron Scout. *Cornea* 2001;20:859–863.
6. Price FW Jr, Whitson WE, Collins KS, Marks RG. Five-year corneal graft survival. A large, single-center patient cohort. *Arch Ophthalmol* 1993;111:799–805.
7. Greenbaum A, Hasany SM, Rootman D. Optisol vs Dextol as storage media for preservation of human corneal epithelium. *Eye* 2004;18:519–524.
8. Bald MR, Stoeger C, Galloway J, Tang M, Holiman J, Huang D. Use of Fourier-domain optical coherence tomography to evaluate anterior stromal opacities in donor corneas. *J Ophthalmol* 2013;397680 [Epub 28 Mar 2013].
9. Huang D, Swanson EA, Lin CP, Schuman JS, Stinson WG, Chang W, et al. Optical coherence tomography. *Science* 1991;254:1178–1181.
10. Swanson EA, Izatt JA, Hee MR, Huang D, Lin CP, Schuman JS, et al. *In vivo* retinal imaging by optical coherence tomography. *Opt Lett* 1993;18:1864–1866.
11. Izatt JA, Hee MR, Swanson EA, Lin CP, Huang D, Schuman JS, et al. Micrometer-scale resolution imaging of the anterior eye *in vivo* with optical coherence tomography. *Arch Ophthalmol* 1994;112:1584–1589.
12. Dubois A, Grieve K, Moneron G, Lecaque R, Vabre L, Boccara C. Ultrahigh-resolution full-field optical coherence tomography. *Appl Opt* 2004;43:2874–2883.
13. Grieve K, Paques M, Dubois A, Sahel J, Boccara C, Le Gargasson JF. Ocular tissue imaging using ultrahigh-resolution, full-field optical coherence tomography. *Invest Ophthalmol Vis Sci* 2004;45:4126–4131.
14. Akiba M, Maeda N, Yumikake K, Soma T, Nishida K, Tano Y, Chan KP. Ultrahigh-resolution imaging of human donor cornea using full-field optical coherence tomography. *J Biomed Opt* 2007;12:041202.

15. Latour G, Georges G, Lamoine LS, Deumié C, Conrath J, Hoffart L. Human graft cornea and laser incisions imaging with micrometer scale resolution full-field optical coherence tomography. *J Biomed Opt* 2010;15:056006.
16. Casadessus O, Georges G, Lamoine LS, Deumié C, Hoffart L. Light scattering from edematous human corneal grafts' microstructure: experimental study and electromagnetic modelization. *Biomed Opt Express* 2012;3:1793–1810.
17. Borderie VM, Scheer S, Touzeau O, Védie F, Carvajal-Gonzalez S, Laroche L. Donor organ cultured corneal tissue selection before penetrating keratoplasty. *Br J Ophthalmol* 1998;82:382–388.
18. Dubois A, Vabre L, Boccara AC, Beaurepaire E. High-resolution full-field optical coherence tomography with a Linnik microscope. *Appl Opt* 2002;41:805–812.
19. Grieve K, Dubois A, Simonutti M, Paques M, Sahel J, Le Gargasson JF, Boccara C. In vivo anterior segment imaging in the rat eye with high speed white light full-field optical coherence tomography. *Opt Express* 2005;13:6286–6295.
20. Assayag O, Antoine M, Sigal-Zafrani B, Riben M, Harms F, Burcheri A, et al. Large field, high resolution full-field optical coherence tomography: a pre-clinical study of human breast tissue and cancer assessment. *Technol Cancer Res Treat* 2014;13:455–468.
21. Dalimier E, Salomon, D. Full-field optical coherence tomography: a new technology for 3D high-resolution skin imaging. *Dermatology (Basel)* 2012;224:84–92.
22. Terry MA, Ousley PJ. New screening methods for donor eye-bank eyes. *Cornea* 1999;18:430–436.
23. Priglinger SG, Neubauer AS, May CA, Alge CS, Wolf AH, Mueller A, et al. Optical coherence tomography for the detection of laser in situ keratomileusis in donor corneas. *Cornea* 2003;22:46–50.
24. Lin RC, Li Y, Tang M, McLain M, Rollins AM, Izatt JA, et al. Screening for previous refractive surgery in eye bank corneas by using optical coherence tomography. *Cornea* 2007;26:594–599.
25. Latrive A, Boccara AC. In vivo and in situ cellular imaging full-field optical coherence tomography with a rigid endoscopic probe. *Biomed Opt Express* 2011;2:2897–2904.